Effect of electropulsing treatment on solid solution behavior of an aged Mg alloy AZ61 strip

Yanbin Jiang
Advanced Materials Institute, Graduate School at Shenzhen, Tsinghua University, Shenzhen 518055, People's Republic of China; and Department of Physics and Materials Science, City University of Hong Kong, Kowloon Tong, Hong Kong

Guoyi Tang,[a] Lei Guan, Shaonan Wang, and Zhuohui Xu
Advanced Materials Institute, Graduate School at Shenzhen, Tsinghua University, Shenzhen 518055, People's Republic of China

Chanhung Shek
Department of Physics and Materials Science, City University of Hong Kong, Kowloon Tong, Hong Kong

Yaohua Zhu
Department of Industrial and Systems Engineering, Hong Kong Polytechnic University, Kowloon, Hong Kong

(Received 16 March 2008; accepted 24 June 2008)

The effect of electropulsing treatment (EPT) on the solution behavior of aged Mg alloy AZ61 strip was investigated using scanning electron microscope (SEM) and x-ray diffraction (XRD). It was found that EPT accelerated tremendously the dissolution of β phase into α matrix in an aged Mg alloy AZ61 strip. The dissolution of β phase took place in less than 4 s at relatively low temperature under EPT, compared with that in conventional heat treatment. A mechanism for rapid solid solution process during EPT was proposed based on the coupling of the thermal and athermal effects. The results in this investigation indicated that EPT played an important role in the nonequilibrium microstructural evolution in the alloy. It is supposed that EPT can provide a highly efficient approach for solid solution treatment of the alloy.

I. INTRODUCTION

Electropulsing treatment (EPT), as an instantaneous high-energy input method, has been applied for improving microstructure and properties of materials. It has been reported that applying an electric current pulse during the solidification process refined grain size.[1–5] EPT was also used during annealing of cold-worked copper to obtain fine recrystallized grains and to retard the formation of annealing twins.[6–10] Conrad et al.[6–9] proposed that the high mobility of dislocations due to the electric current played an important role in such effects. In our previous work, complete recrystallization of a cold-worked Mg alloy AZ31 strip was achieved in several seconds at relatively low temperature (483 K) under EPT. In the case of EPT, the recrystallization mechanism could be attributed to the coupled action of thermal and athermal effects.[11] Zhang et al.[12,13] developed an electropulsing treatment for synthesizing nanostructured materials directly from conventional coarse-grained crystalline materials because of the rapid heating/cooling cycle resulting from electropulsing. However, the method of EPT applied to the solid solution treatment of magnesium alloys on-line has not been reported. In the present paper, the influence of EPT on the solid solution behavior of an aged Mg alloy AZ61 strip (AZ61 strip) is reported and the mechanism of the effect is discussed.

II. EXPERIMENTAL

The commercial magnesium alloy AZ61 (6.3 wt% Al, 1.1 wt% Zn, 0.2 wt% Mn, balance Mg) was used. The ingot was homogenized at 673 K for 16 h and subsequently extruded into a strip 2.96 mm wide and 1.5 mm thick. The extruded strip was then cold-rolled to 1.05 mm thick. The cold-worked strip was aged for 12 h at 523 K to obtain the as-aged strip consisting of α-Mg and β-$Mg_{17}Al_{12}$. The samples were divided into three groups, namely, Samples A, Samples AT, and Samples EPT. Samples A were as-aged strips without any treatment. Samples AT were heated up to 643 K in about 5 s in a furnace, and the average heating rate was about

[a]Address all correspondence to this author.
e-mail: tanggy@mail.tsinghua.edu.cn
DOI: 10.1557/JMR.2008.0328

74 K/s. The samples were then cooled in air. Samples EPT were subjected to EPT with various parameters of electropulsing (see Table I).

The entire EPT process is shown schematically in Fig. 1. The AZ61 strip was treated on-line by multiple electropulses, when the strip was moving at a speed of 3.67 m/min through a distance of 225 mm between the two electrodes. Multiple electropulses were produced continuously by the electropulsing generator. During this process, it took about 4 s to move the strip from anode and cathode. The pressure between the electrodes and the strip was sufficient to maintain a good electrical contact without causing deformation of the strip. Electropulses with various frequencies and a small variation in pulse duration of 60–70 μs were applied to the strip. Current parameters, including frequency, root-mean-square current (RMS), amplitude, and duration of current pulses, were monitored by a Hall effect sensor connected to an oscilloscope. The temperature of the AZ61 strip near the cathode, due to the Joule heating effect of EPT, was measured using a Raytek MX2 infrared thermoscope (Raytek Corp., Santa Cruz, CA). Note that Sample EPT7 had an average heating rate of 91 K/s during EPT, which was a similar heating profile to that of Sample AT.

A JSM-820 JEOL scanning electron microscope (SEM) and an optical microscope (OPM) were used to observe the microstructure of the samples (JEOL, Tokyo, Japan). The SEM and OPM samples were polished and etched. Chemical compositions of phases in the samples were examined by energy-dispersive x-ray spectroscopy (INCA 200; Oxford Instruments, Oxford, England) in SEM. The phases in the samples were identified by x-ray diffraction (XRD) with Cu K_α radiation. Vickers hardnesses of all the samples were measured as well.

III. EXPERIMENTAL RESULTS

The relationship between hardness, frequency, and temperature is shown in Table I and Fig. 2. It was observed that the temperature of the EPT samples increased

TABLE I. Experimental conditions of AZ61 strip under EPT.

Sample no.	Frequency (Hz)	Duration (μs)	j_m (A/mm^2)	j_e (A/mm^2)	Temperature (K)
EPT1	200	68	334	27.7	484
EPT2	248	68	334	30.6	511
EPT3	306	68	342	34.7	559
EPT4	361	68	329	37.1	603
EPT5	387	68	329	38.6	613
EPT6	402	68	329	39.1	628
EPT7	451	68	338	42.0	638
EPT8	481	68	334	43.1	653

Note: j_m is the amplitude of current density of electropulsing, and j_e represents the RMS value of current density during EPT and is related to the Joule heating effect.

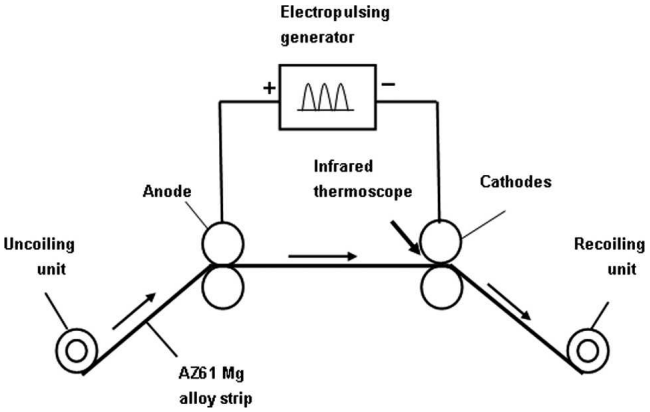

FIG. 1. Schematic view of the EPT process.

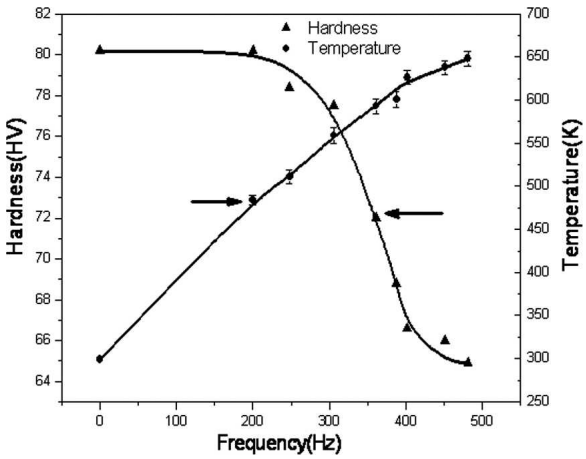

FIG. 2. Relationship between hardness, temperature, and frequency of electropulsing of samples.

gradually with frequency due to the Joule heating effect. The higher frequency contributed to a larger RMS value of current density, which resulted in a larger Joule heating effect. Sample hardness was strongly influenced by frequency and temperature. The β phase transformed to the α phase rapidly in about 4 s, when the temperature of the EPT sample was over 578 K,[14] i.e., the phase-transformation temperature. This phase transformation resulted in decreasing hardness of the EPT samples. Additionally, the decrease in hardness could partly ascribe to the grain growth when electropulsing frequency exceeded 402 Hz. However, hardness of the AT sample by conventional heat treatment retained its high value of about 76 HV, which was close to that of the EPT sample with a pulse frequency of 306 Hz.

Shown in Fig. 3 are the XRD patterns of the samples under different conditions. One can see that Sample A consists of mainly two phases: α-Mg and β-$Mg_{17}Al_{12}$. With increasing electropulsing frequency, the peaks of β-$Mg_{17}Al_{12}$ weakened and vanished when the frequency increased to 402 Hz. This means that decomposition of the β-$Mg_{17}Al_{12}$ occurred gradually with increasing

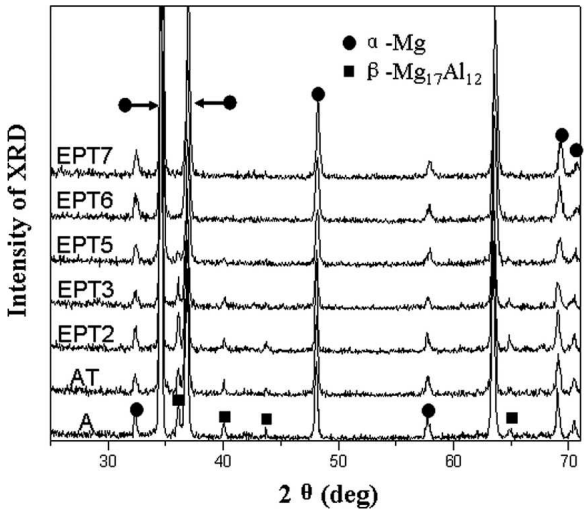

FIG. 3. XRD patterns for samples at various conditions.

frequency of electropulsing during EPT. It was found that the position of the α-Mg peaks shifted toward a high diffraction angle, as shown in Fig. 3. The lattice parameter *a* of α-Mg, calculated from Bragg angles in Fig. 3, was reduced gradually when the frequency of electropulsing increased (see Fig. 4). It is supposed that Al atoms of the β-$Mg_{17}Al_{12}$ underwent significant long-range diffusion into the α-Mg within a very short time—on the order of seconds—during EPT. However, XRD analysis shows that the β-$Mg_{17}Al_{12}$ still existed in the AT sample by conventional heat treatment, which had a heating profile similar to that of EPT, with a frequency of 451 Hz.

Figure 5 shows the optical microstructure of the as-extruded sample and the cold-rolled sample. Equiaxed grains averaging about 10 μm were observed in the as-extruded sample [Fig. 5(a)]. The typical microstructure

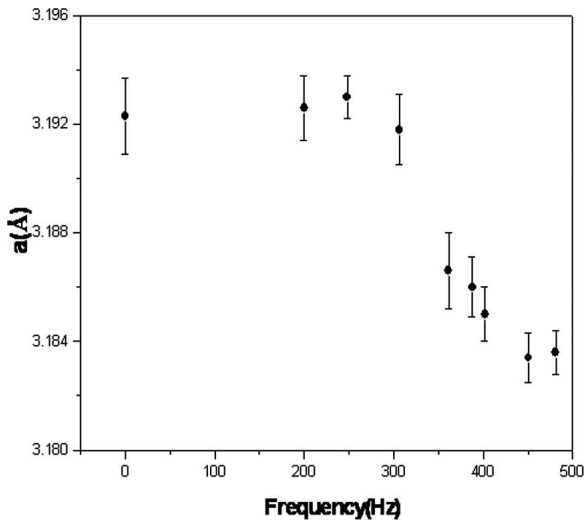

FIG. 4. Variation of lattice parameter *a* of α-Mg matrix with electropulsing frequencies.

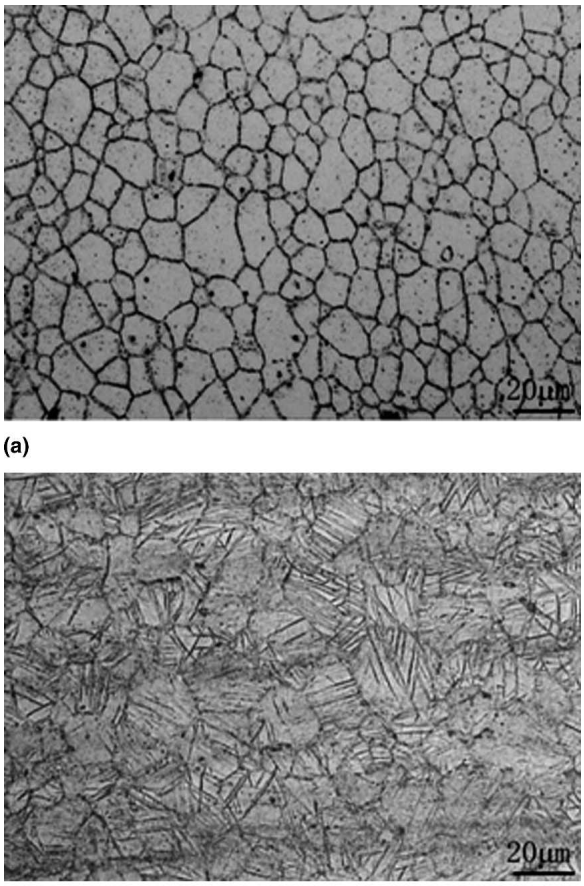

FIG. 5. Optical microstructure of samples: (a) as-extruded sample; (b) cold-rolled sample.

of cold-rolled Mg alloy with many twins inside the grains was observed in the cold-rolled sample [Fig. 5(b)]. Figure 6 gives the SEM micrographs of the samples treated with different conditions. The matrix was α-Mg and the precipitates were β-$Mg_{17}Al_{12}$ [Fig. 6(a)]. From EDS analysis, the compositions of the matrix and the precipitates were 92.8 wt% Mg–5.7 wt% Al–1.5 wt% Zn and 60.8 wt% Mg–39.2 wt% Al, which were close to the nominal compositions of the α and β phases, respectively. During the aging process, a number of small precipitates of β phase formed inside grains while large precipitates of β phase were formed at grain boundaries. This agreed well with the result of Duly et al.[15] From Figs. 6(b)–6(e), different extents of transformations from β phase to α phase are observed with changes in the frequency of electropulsing. Increasing the frequency of electropulsing accelerated the transformation from β phase to α phase, and phase transformation was close to completion at the frequencies of 402 and 451 Hz; however, there were few β phase particles undissolved in Sample EPT7 [Figs. 6(d) and 6(e)]. In addition, slight grain growth occurred, due to dissolution of the β phase

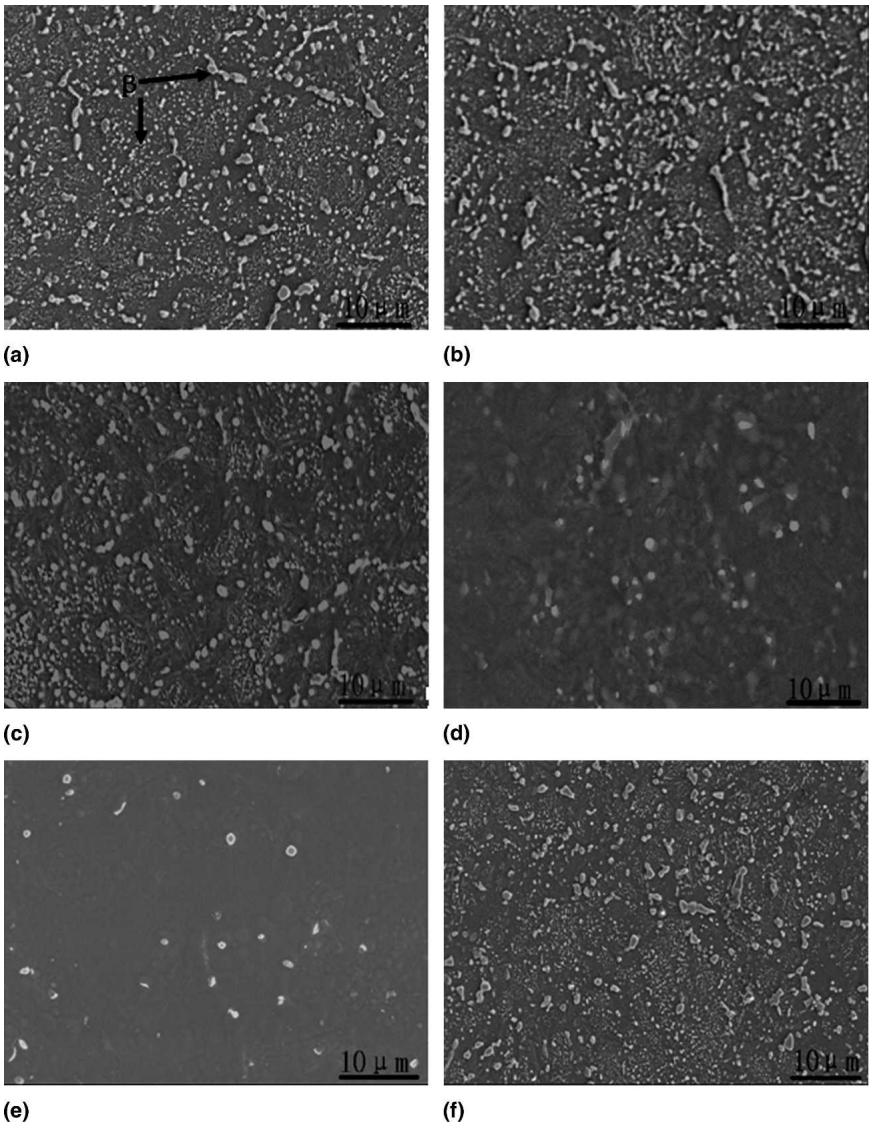

FIG. 6. SEM micrographs of samples: (a) Sample A (as-aged); (b) Sample EPT3 (306 Hz); (c) Sample EPT4 (361 Hz); (d) Sample EPT6 (402 Hz); (e) Sample EPT7 (451 Hz); (f) Sample AT.

particles at the grain boundaries, when electropulsing frequency exceeded 402 Hz. Referring to Table I and Fig. 3, it is revealed that, under EPT, the phase transformation is initiated at relatively low temperature and that the transformation was complete within a short time compared with that in conventional heat treatment. However, numerous β-$Mg_{17}Al_{12}$ particles remained in the Sample AT (by conventional heat treatment) [see Fig. 6(f)]. SEM results were in good agreement with the XRD analysis.

IV. DISCUSSION

The local vertical section of the phase diagram pertinent to Mg–6 wt% Al–Zn alloys shows that the solvus temperature of β → α for the experimental alloy is about 578 K, as shown in Fig. 7.[14] It means that β-$Mg_{17}Al_{12}$ transforms to α-Mg when the temperature is higher than 578 K, if long-range diffusion of atoms can be achieved. In Table I, the temperatures of the EPT samples (EPT4–EPT8) were higher than 578 K, which indicated that the phase transformation β → α could take place during the rapid heating process of EPT.

Figure 6 shows the microstructural evolution of AZ61 with increasing frequency during EPT. It was obvious that increasing frequency of electropulsing accelerated tremendously the solid-phase transformation, β → α. However, it was intriguing that the microstructural change of the EPT sample at 451 Hz was different from that of the AT sample (by conventional heat treatment) [see Figs. 6(e) and 6(f)], even though they had similar rapid heating profiles. It must be pointed out that the phase transformation, β → α, is a diffusional phase

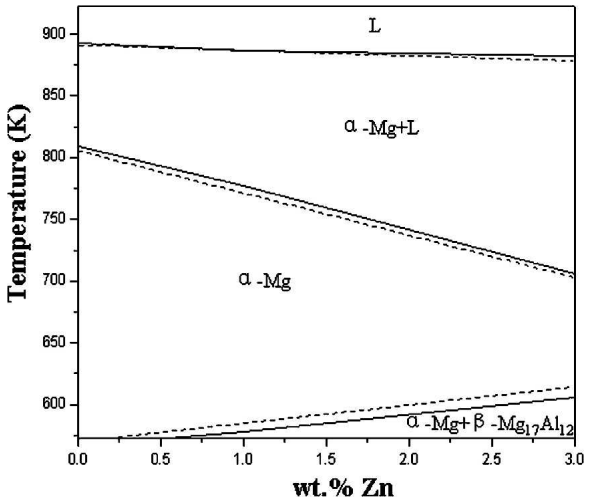

FIG. 7. Local vertical section of phase diagram of Mg–Al6–Zn alloys; solid lines for nominal 6.0 wt% Al, dotted lines for 6.24 wt% Al.[14]

transformation, which cannot occur without long-range diffusion, even when the thermodynamic conditions are satisfied. This implied that EPT accelerated long-range diffusion considerably compared with conventional heat treatment. With EPT, it took only 4 s to complete the diffusional phase transformation in the as-aged AZ61 strip. Previous studies[16–18] indicated that the effect of electric current on the atomic drift flux of atoms in metals can be described by Nernst–Einstein equation.

$$J_i = \frac{N_i \cdot D_i}{kT}\left(kT \cdot \frac{\partial \ln X_i}{\partial x} - \Omega \cdot \frac{\partial \sigma}{\partial x} + Z^* \cdot e \cdot \rho \cdot j\right) \quad , \qquad (1)$$

where N_i is the density of ith atom species, D_i is the pertinent diffusion coefficient, Z^* an effective valence, e the charge on an electron, ρ the resistivity, j the current density, X_i the concentration of the ith solute, Ω the atom volume, $-\partial\sigma/\partial x$ the stress gradient, k the Boltzmann constant, and T the absolute temperature. In Eq. (1), the first term in brackets is due to the composition gradient, the second term is due to the chemical potential gradient between vacancies and atoms in the system, and the third term arises from the interaction between electrons and atoms. However, the exact mechanism of how electric current influences the mobility of atoms is still not clear. Here, one possible explanation for the effect of electropulsing on the drift flux of atoms J is based on the coupling of thermal effect J_t and athermal effect J_a,[10] where J_t is the flux of atoms resulting from thermal activated effect during the rapid heating process of EPT[19] and J_a is the flux of atoms contributed by athermal effects of EPT.

$$J_t = \frac{2\pi D_l}{\Omega \ln\left(\frac{R}{r_0}\right)} \cdot \left(1 + \frac{\delta c}{c_0}\right)$$

$$J_a = \frac{N \cdot D_l \cdot Z^* \cdot e \cdot \rho \cdot j}{kT}$$

$$J = J_t + J_a = \frac{2\pi D_l}{\Omega \ln\left(\frac{R}{r_0}\right)} \cdot \left(1 + \frac{\delta c}{c_0}\right) + \frac{N \cdot D_l \cdot Z^* \cdot e \cdot \rho \cdot j}{kT} \quad , \qquad (2)$$

where D_l is the lattice diffusion coefficient, c_0 the average concentration of vacancy, δc the supersaturation concentration of vacancies, r_0 and R the distances far from dislocation where the vacancy concentrations are c_0 and $c_0 + \delta c$, respectively; Z^*, e, ρ, j, Ω, k, and T have the same meanings as in Eq. (1). J_t is the flux of vacancies resulting from the thermal effect of EPT, and the flux of atoms resulting from the thermal effect can be equivalent to the flux of vacancies resulting from the thermal effect because Mg alloy AZ61 is a substitutable solid solution. J_a is the flux of atoms due to the interaction between electrons and atoms, namely, the athermal effect of EPT. However, Eq. (2) is suitable for the flux of atoms resulting from a constant current because only the constant current density j affects the total atomic flux. In the case of electropulsing, current is on and off alternately. Therefore, frequency f and duration τ_p of electropulsing should also affect the atomic flux. To simplify the problem, the pulse shape is taken as half-sine curve, as shown in Fig. 8. Current density of electropulsing can be represented by Eq. (3).

$$j = \begin{cases} j_m \cdot \sin\left(\frac{\pi}{\tau_p} \cdot t\right), & 0 < t < \tau_p \\ 0, & \tau_p < t < t_p \end{cases} \quad . \qquad (3)$$

Substituting Eq. (3) into Eq. (2) gives the following formulae for the instantaneous atomic flux contributed from electropulsing:

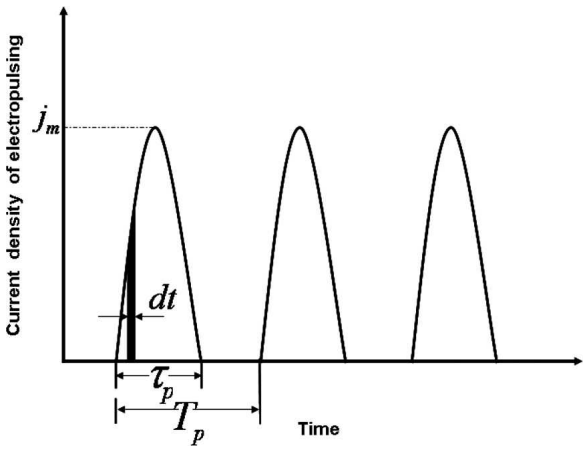

FIG. 8. Waveform of electropulsing.

$$J = \begin{cases} \dfrac{2\pi D_l}{\Omega \ln\left(\dfrac{R}{r_0}\right)} \cdot \left(1 + \dfrac{\delta c}{c_0}\right) + \dfrac{N \cdot D_l \cdot Z^* \cdot e \cdot \rho \cdot j_m \cdot \sin\left(\dfrac{\pi}{\tau_p} \cdot t\right)}{KT}, & 0 < t < \tau_p \\ \dfrac{2\pi D_l}{\Omega \ln\left(\dfrac{R}{r_0}\right)} \cdot \left(1 + \dfrac{\delta c}{c_0}\right), & \tau_p < t < t_p \end{cases} . \quad (4)$$

Integrating Eq. (4) will give the average atomic flux per second during multiple continuous electropulses passing through the AZ61 strips in Eq. (5).

$$J = \frac{2\pi D_l}{\Omega \ln\left(\dfrac{R}{r_0}\right)} \cdot \left(1 + \frac{\delta c}{c_0}\right) + \frac{2N \cdot D_l \cdot Z^* \cdot e \cdot \rho \cdot f \cdot j_m \cdot \tau_p}{\pi k T} . \quad (5)$$

According to Eq. (5), the average atomic flux increases tremendously due to the athermal effect J_a resulting from electropulsing, which is an additional energy input compared with conventional heat treatment. In other words, with the aid of electropulsing, it is possible that the average atomic flux in the alloy is sufficient to accelerate diffusional phase transformation at relatively low temperature in a short period of time. Additionally, Eq. (5) also reveals that J_a is strongly dependent on the parameters of electropulsing and increases linearly with frequency f, duration τ_p, and peak current density j_m when the temperature T is constant. During EPT, the sample temperature due to the Joule heating effect increases with these three parameters if the other physical parameters of the sample remain uncharged. Therefore, increasing f, τ_p, and j_m not only enhances athermal effect but also increases the thermal effect. The temperature of the samples is an important factor during EPT, and this can be evidenced in the microstructural evolution of the samples during EPT, where only the frequency of electropulsing changed, as shown in Figs. 3 and 6(b)–6(e). There were many β phase particles in Samples AE2 (248 Hz) and AE3 (306 Hz), and the diffusional phase transformation seemed not to happen substantially. However, by only increasing frequency to 402 Hz or 450 Hz, a large amount of β-phase particles disappeared because of the diffusional phase transformation with long-range diffusion of Al solute into Mg matrix. Apparently, increasing the frequency enhances the atomic flux due to athermal effects, as in Eq. (5). However, when only the effect of frequency on the atomic flux is taken into account, the dissolution rate of β-phase particles in the Mg matrix cannot be explained satisfactorily because the electropulsing frequency change of 150 Hz does not affect athermal effect much, as shown in Eq. (5). Actually, temperature is another important factor for the atomic flux in the case of EPT because D_l increases exponentially with temperature T; see Eq. (6)[20]:

$$D_l = D_0 \exp\left(\frac{-Q}{RT}\right) , \quad (6)$$

where D_0 is the diffusion pre-exponential factor, Q the activation energy, and R the gas constant. From the above analysis, electropulsing tremendously enhances the atomic flux and accelerates the diffusional phase transformation at an adequate temperature during EPT. In addition, because the properties of the α and β phases are different, their local temperature resulted from Joule heating effect may be different. The local temperature gradient could contribute to an atomic flux due to thermotransport. However, Hummel[21] proposed that thermotransport is a second-order effect compared with that of electromigration. Furthermore, EPT in the present work can be considered simply as a nonequilibrium process of heating/cooling cycles. The equilibrium vacancy concentration is sensitive to temperature and is frequently upset by electropulsing. Compared with conventional heat treatment, this may enhance the amount of vacancies and activate their mobility dramatically. In general, atoms in metal always vibrate about their equilibrium position at a certain frequency ν, whereas electropulsing may increase the probability of creating vacancies around vibrational atoms. It means that the rate of atoms jumping into vacancies may be increased remarkably, once the atoms obtain enough energy from electropulsing. This may result in increasing the change of activation entropy ΔS in the alloy. Therefore, the diffusion pre-exponential factor D_0 increases by $D_0 = f' a^2 \nu \exp(\Delta S/k)$,[20] where f' is a constant for a certain system and a is the lattice constant. Previous study[22] has even shown that increasing diffusion coefficient due to electropulsing was partly attributed to the reduction of the activation energy Q, which resulted from a decrease in the strength of the opposing atom motion and an increase in the defect density.

The experimental results in the present study can be

explained on the basis of the coupling effect of thermal and athermal effects on the dissolution of β-phase particles in Mg alloy AZ61. However, further clarification of the exact mechanism of EPT on the phase transformation should be done in the future, including determination of the relative contributions of J_t and J_a.

On the basis of the experimental results and analysis above, EPT can effectively accelerate the solid solution behavior of the aged AZ61 strip compared with conventional heat treatment. In general, at least 30 min is needed to complete conventional solid solution heat treatment of AZ61 strips at a range of 673–693 K. EPT effectively inputs instantaneous high-energy directly to the lattice of the Mg alloy, and a large amount of β-phase precipitates at relative low temperature (about 628 K) were dissolved after several seconds of EPT. This means that EPT can save a great deal of energy and time for solid solution treatment of AZ61 strips compared with conventional heat treatment. Therefore, it is proposed that EPT may provide a highly efficient approach for solid solution treatment of alloys in the engineering field.

V. CONCLUSIONS

(1) The diffusional phase transformation, $\beta \rightarrow \alpha$, took place in the aged Mg alloy AZ61 strip after EPT for 4 s, while no substantial diffusional phase transformation was found in conventional heat treatment with the similar heating profile as EPT.

(2) Compared with conventional heat treatment, EPT accelerated the diffusional phase transformation, $\beta \rightarrow \alpha$, of the aged AZ61 because of the tremendous increase in the atomic flux resulting from coupling of thermal and athermal effects. An adequate thermal effect resulting from the Joule heating effect of EPT should be necessary for effective use of the athermal effect due to the interaction between electrons and atoms.

(3) EPT provides a highly efficient approach for solid solution treatment of magnesium alloy sheets/strips.

ACKNOWLEDGMENTS

The authors acknowledge support from the Tsinghua–CityU Collaboration Scheme. The work was supported by the National Natural Science Foundation of China (No. 50571048).

REFERENCES

1. A.K. Misra: A novel solidification technique of metals and alloys under the influence of applied potential. *Metall. Trans. A* **16,** 1354 (1985).
2. A.K. Misra: Misra technique applied to solidification of cast-iron. *Metall. Trans. A* **17,** 358 (1986).
3. M. Nakada, Y. Shiohara, and M.C. Flemings: Modification of solidification structures by pulse electric discharging. *ISIJ Int.* **30,** 27 (1990).
4. M. Gao, G.H. He, F. Yang, J.D. Guo, Z.X. Yuan, and B.L. Zhou: Effect of electric current pulse on tensile strength and elongation of casting ZA27 alloy. *Mater. Sci. Eng., A* **337,** 110 (2002).
5. J.P. Barnak, A.F. Sprecher, and H. Conrad: Colony (grain) size reduction in eutectic Pb–Sn casting by electropulsing. *Scr. Metall. Mater.* **32,** 879 (1995).
6. H. Conrad, N. Karam, and S. Mannan: Effect of electric-current pulses on the recrystallization of copper. *Scr. Metall.* **17,** 411 (1983).
7. H. Conrad, N. Karam, and S. Mannan: Effect of prior cold work on the influence of electric-current pulses on the recrystallization of copper. *Scr. Metall.* **18,** 275 (1984).
8. H. Conrad, N. Karam, S. Mannan, and A.F. Sprecher: Effect of electric-current pulses on the recrystallization kinetics of copper. *Scr. Metall.* **22,** 235 (1988).
9. H. Conrad, Z. Guo, and A.F. Sprecher: Effects of electropulse duration and frequency on grain-growth in Cu. *Scr. Metall.* **24,** 359 (1990).
10. Z.H. Xu, G.Y. Tang, S.Q. Tian, and J.C. He: Research on the engineering application of multiple pulses treatment for recrystallization of fine copper wire. *Mater. Sci. Eng., A* **424,** 300 (2006).
11. Z.H. Xu, G.Y. Tang, F. Ding, S.Q. Tian, and H.Y. Tian: The effect of multiple pulse treatment on the recrystallization behavior of Mg–3Al–1Zn alloy strip. *Appl. Phys. A* **88,** 429 (2007).
12. W. Zhang, M.L. Sui, Y.Z. Zhou, and D.X. Li: Evolution of microstructures in materials induced by electropulsing. *Micron* **34,** 189 (2003).
13. W. Zhang, M.L. Sui, K.Y. Hu, D.X. Li, X.N. Guo, G.H. He, and B.L. Zhou: Formation of nanophases in a Cu-Zn alloy under high current density electropulsing. *J. Mater. Res.* **15,** 2065 (2000).
14. M. Ohno, D. Mirkovic, and R. Schmid-Fetzer: Phase equilibria and solidification of Mg-rich Mg–Al–Zn alloys. *Mater. Sci. Eng., A* **421,** 328 (2006).
15. D. Duly, M. Audier, and Y. Brechet: On the influence of plastic-deformation on discontinuous precipitation in Mg–Al. *Scr. Metall.* **29,** 1593 (1993).
16. H. Conrad: Effect of electric current on solid-state phase transformations in metals. *Mater. Sci. Eng., A* **287,** 227 (2000).
17. I.A. Blech: Electromigration in thin aluminum films on titanium nitride. *J. Appl. Phys.* **47,** 1203 (1976).
18. E. Kinsbron: A model for the width dependence of electromigration lifetimes in aluminum thin-film stripes. *Appl. Phys. Lett.* **36,** 968 (1980).
19. Z.H. Xu: Applied fundamental research of the high-density pulses on the processing of wrought magnesium alloy thin strip. Ph.D. Thesis, Beijing, Tsinghua University, 2007, p. 61.
20. D.A. Porter and K.E. Easterling: *Phase Transformations in Metals and Alloys*, 2nd ed. (Chapman & Hall, London, 1992), p. 68.
21. R.E. Hummel: Electromigration and related failure mechanisms in integrated-circuit interconnects. *Int. Mater. Rev.* **39,** 97 (1994).
22. Y.Z. Zhou, W. Zhang, J.D. Guo, and G.H. He: Diffusive phase transformation in a Cu–Zn alloy under rapid heating by electropulsing. *Philos. Mag. Lett.* **84,** 341 (2004).